



Characterization of HILDCAA events using Recurrence Quantification Analysis

Odim Mendes¹, Margarete Oliveira Domingues², Ezequiel Echer¹, Rajkumar Hajra^{1,3}, and Varlei Everton Menconi¹

¹Space Geophysics Division (DGE/CEA), Brazilian Institute for Space Research (INPE), São José dos Campos, São Paulo, Brazil.

²Associated Laboratory of Computation and Applied Mathematics (LAC/CTE), Brazilian Institute for Space Research (INPE), São José dos Campos, São Paulo, Brazil.

³Laboratoire de Physique et Chimie de l'Environnement et de l'Espace (LPC2E), CNRS, Orléans 45100, France.

Correspondence to: Odime Mendes (odim.mendes@inpe.br)

Abstract. Taking into account the primary mechanisms for transfer particles and energy into the magnetosphere, we have studied the dynamical characteristics of High-Intensity Long-Duration Continuous Auroral Activity (HILDCAA) events using a long-term geomagnetic database (1975-2012). The Recurrence Quantification Analysis method was applied on the auroral electrojet indices during HILDCAA events to characterize their dynamics. After, we compared those results with the ones obtained for geomagnetically quiet periods when there was no appreciable auroral activity. As result, the quantification allowed to find specific characteristics of these two distinct regimes. The HILDCAA events can be described as unique processes responsible for complex transfers of energy and particles from the solar wind plasmas into the magnetosphere-ionosphere system. We also suggest that the scenario of these processes is related to concurrent magnetospheric mechanisms (magnetic reconnection and viscous interaction). At last, we reinforce the potential applicability of the RQA method for characterization of various nonlinear geomagnetic processes related to these phenomenology.

1 Introduction

As well known currently, a complicated electrodynamical region — designated as magnetosphere — populated by plasmas and ruled by the Earth's magnetic field exists surrounding our planet (Mendes et al., 2005; Kivelson and Russell, 1995). This region is exposed to influences of space environment and submitted to several interplanetary forcings. In a summary view, a physical scenario could be properly interpreted according to the following description.

In electrodynamic terms, three main solar agents (electromagnetic radiation, high energetic particles and solar magnetized structures) act upon the Earth's atmosphere, which is permeated by a magnetic field created in the interior of our planet (Campbell, 2003; Hargreaves, 1992). Initially electromagnetic radiation both heats globally the planet and ionizes the atmosphere. This ionization gives basis to a terrestrial plasma environment. Also, the incidence episodes of solar high energetic particles increase the ionization in a manner much more localized. At last, escaping in a continuous way from the Sun, the solar wind



superposed sometimes by coronal mass ejections structures and other peculiar solar structures (e. g., solar fast speed streams and heliospheric current sheet), transport intrinsically a solar magnetic field and reaches the orbit of the Earth.

Two primary electrodynamic interactions are possible from this incidence of the magnetized solar plasma upon the Earth's magnetosphere. Those interactions transfer energy and particles into the magnetosphere boundary. The most intense is through the magnetic reconnection (Burch and Drake, 2009; Kivelson and Russell, 1995), when the Interplanetary Magnetic Field (IMF) merges into the geomagnetic field at the outer boundary. It is an efficient process of energy and particle transfers. The reconnection process occurs when IMF presents a predominantly southward orientation and creates strong alterations in a large region formed by the magnetosphere and the ionosphere, a region about 100 to 2000 km of altitude presenting the highest quantity of ionized particles. Another competitive process is the Kelvin-Helmholtz viscous interaction (Hasegawa et al., 1997; Chen et al., 2004). Most of the time this second process is in action when the magnetosphere acts as a closed physical system with respect to incident frontal solar wind. The fluid dynamics developed by the plasma sliding at the flanks of the magnetosphere creates a kind of viscous interaction, which produces the mixing of the solar plasma inside the magnetosphere and the occurrence of ULF waves (Menk and Waters, 2013) affecting the interior regions.

In a global wide sense, during events of solar wind transporting interplanetary magnetic field parallel to the frontal geomagnetic field, a regime of low magnetic disturbance on ground is noticed. However, when the interplanetary magnetic field is strongly southward directed, anti parallel to the geomagnetic field, strong regimes of disturbances are recorded on ground. But there is a peculiar interplanetary process related to manifestations of Alfvén waves, with alternating of the magnetic component orientation, which produce an intermediate level of geomagnetic disturbance with typically duration of days, as analyzed in Guarnieri et al. (2006).

The interplanetary nonlinear Alfvén waves are known to be the main origin of high-intensity long-duration continuous *AE* activity (HILDCAA) events on the Earth (Tsurutani and Gonzalez, 1987; Tsurutani et al., 1990, 2011b, a; Echer et al., 2011; Hajra et al., 2013). The geomagnetic index *AE* represents the quantification of the geomagnetic disturbance produced by enhanced ionospheric electric currents flowing below and within the auroral oval (<https://www.ngdc.noaa.gov/stp/geomag/ae.html>). The primary mechanism for the events is as follows. The high-speed solar wind streams (HSSs) emanating from solar coronal holes are accompanied by embedded Alfvén waves (Belcher and Davis, 1971; Tsurutani et al., 1994). The waves are characterized by large interplanetary magnetic field (IMF) variability $\Delta B/B_0 \sim 1$ to 2 (ΔB being the peak-to-peak amplitude of the transverse magnetic field and B_0 is the IMF magnitude) (see Echer et al. (2011, 2012); Tsurutani et al. (2011b, a)). The sporadic magnetic reconnection (Dungey, 1961; Gonzalez and Mozer, 1974) between the southward component of the Alfvén waves and the Earth's magnetopause fields leads to the intense substorm/convection events comprising HILDCAAs (Tsurutani et al., 1995). The events are shown to last from days to weeks (Tsurutani et al., 1995, 2006; Gonzalez et al., 2006; Guarnieri, 2006; Kozyra et al., 2006; Hajra et al., 2013, 2014a).

As a major feature, the HILDCAA events carry a large amount of solar wind kinetic energy input into the magnetosphere (Gonzalez et al., 2006; Hajra et al., 2014b). More than 60% of this energy is dissipated in the outer magnetosphere-ionosphere system. Additionally, recent studies show that these events are related to the acceleration of relativistic electrons in the Earth's



radiation belts (Hajra et al., 2014c, 2015b, a). These are known as “killer electrons” for their hazardous effects to orbiting spacecraft (Wrenn, 1995; Horne, 2003).

Like most of the geomagnetic processes, HILDCAAs represent nonlinear processes. The variations of AE during HILDCAAs capture the nonlinear dynamics of the physical processes in the presence of noise and a non-stationary behavior. The dynamical characterization of those kinds of phenomena is of fundamental interest for a deeper insight into the related electrodynamic coupling between the solar wind and the geomagnetic processes.

The aim of this work is to highlight characteristics related to the HILDCAA events revealed by the geomagnetic index AE . Thus, a primary question is addressed here. Should the HILDCAA event be understood as a well defined process? I. e., do the HILDCAA physical criteria characterize a unique phenomenon? For this purpose, the recurrence quantification analysis, RQA (Trulla et al., 1996), based on the recurrence plot (Eckmann et al., 1987; Maizel and Lenk, 1981), is then applied. It constitutes a proper tool to treat non linear, non stationary signals. Such analysis method is applied to the geomagnetic activity processes related to HILDCAAs, for the first time to our knowledge. We will describe this robust method and present its potential applicability for these geomagnetic processes later in this paper.

The content of this work is presented as follows. Section 2 describes the methods for analysis, followed by the geomagnetic database and how we applied methodology, on Section 3. Section 4 presents the results and interpretations. Section 5 summarize the conclusions.

2 Method of Analysis

The information theory, as proposed by the mathematician Claude E. Shannon, is based on the mathematical entropy equation (Cover and Thomas, 2006):

$$H(\mathbf{X}) = - \sum P(x) \log(P(x)), x \in \mathbf{X}, \quad (1)$$

where \mathbf{X} is the set of all messages $\{x_1, \dots, x_n\}$ that \mathbf{X} could be, and $p(x)$ is the probability of some $x \in \mathbf{X}$. On this work, we are interested in quantification methods based on this theory, specifically the method of Recurrence Quantification Analysis developed by Zbilut and Webber Jr. (1992) that is build from the Recurrence Plot. On the following we present briefly these methods.

Recurrence Plot (RP)

The Recurrence Plot is based on the Poincaré’s recurrence theorem from 1890 as discussed in Schulman (1978). This theorem states that a dynamic system returns to a state arbitrarily close to the initial state after a certain time. The RP is defined as a square matrix of points that indicates the proximity of two states in the phase space considering a proximity definition (Eckmann et al., 1987). The phase space is formed by coordinates that represent each necessary variable in order to specify an instantaneous state of a system (Marwan, 2003). According to Takens (1981), a close approximation of the phase space can be rebuilt based on the original system and it preserves some geometric invariant of the system. Then, mathematically, RP is obtained by the matrix $\mathbf{R}_{i,j} = \Theta(\epsilon_i - \| \mathbf{x}_i - \mathbf{x}_j \|)$, where ϵ_i is a predefined cut-off distance, $\| \cdot \|$ is the norm (in our case,



the Euclidian norm) and $\Theta(x)$ is the Heaviside function. The values one and zero in this matrix are translated respectively to black and white representation patterns. According to Takens' embedding theorem (Takens, 1981), a reconstruction of the phase space trajectory $\mathbf{x}(t)$ from a time series u_k , with a cadence Δt , allows to present a proper dynamics of a system. In order to do that, an embedding dimension m and a time delay τ must be identified, related to the following reconstruction:

5 $\mathbf{x}(i) = \mathbf{x}_i = (u_i, u_{i+\tau}, \dots, u_{i+(m-1)\tau})$, where $t = i\Delta t$. Here, m is found by using the false nearest neighbour method and τ by the mutual information method (Marwan and Webber, 2015).

Recurrence Quantification Analysis (RQA)

Quantification measurements come basically from the recurrence point density, diagonal structures, and vertical structures in the recurrence plot. Trulla et al. (1996) addressed the problem of quantifying the structure that appears in the RPs and used

10 them to analyse experimental data. This approach is useful to reveal qualitative transitions in a system. The corresponding measurements capture the dynamical characters of the system but represented by the signal. Therefore, the RQA measures provide a qualitative description of a system in terms of complexity measures (Marwan et al., 2007). The diagonal structures in the RP and the recurrence point density are used to measure the complexity of a physical system (Zbilut and Webber Jr., 1992; Webber Jr. and Zbilut, 1994). A more detailed discussion on this subject is presented in Marwan and Kurths (2002), and

15 Marwan (2003). In the present work we restrict our analysis to four characteristic parameters described below:

1. **Recurrence rate (RR)**: It denotes the overall probability that a certain state recurs.
2. **Determinism (DET)**: It represents how predictable a system is.
3. **Laminarity (LAM)**: It measures the occurrence of laminar states and is related to intermittent regimes. This measurement is relatively more robust against noise in signals.
- 20 4. **Entropy (ENTR)**: It reflects the complexity of the deterministic structure in the system based on Shannon entropy (Shannon, 1964). However, it may change for different realizations of the same process or for different data preparations.

We use the RQA tools provided in **Cross Recurrence Plot Toolbox 5.21 (R31b)** by the Interdisciplinary Center for Dynamics of Complex Systems, University of Potsdam (<http://tocsy.pik-potsdam.de/CRPtoolbox/>).

3 Database and Methodology

- 25 For the present work, we have considered an updated list of 136 HILDCAA events occurring between 1975 and 2012, compiled by Hajra et al. (2013). The events were detected from the geomagnetic *AE* and, middle to low latitude disturbance, *Dst* indices by using the the four strict HILDCAA criteria (Tsurutani and Gonzalez, 1987): (i) the events have peak *AE* intensities greater than 1000 nT, (ii) the events last for more than 2 days, (iii) high auroral activity lasts throughout the interval, i.e., *AE* never drops below 200 nT for more than 2 h at a time, and (iv) the events take place outside of a geomagnetic storm main phase.
- 30 To a better understanding, the main phase is determined by the depression in the horizontal component, from middle to low latitudes, in the geomagnetic field. This behavior is identified e quantified by means of the hourly value equatorial *Dst* index,



which represents ideally the axially symmetric disturbance magnetic field at the dipole equator on the Earth's surface. This index is derived monitoring the equatorial ring current variations (<http://wdc.kugi.kyoto-u.ac.jp/dst/dir/dst2/onDstindex.html>). The dataset *AE* is provided by the OMNIweb Service (<http://omniweb.gsfc.nasa.gov/>) by NASA and *Dst* from World Data Center for Geomagnetism, Kyoto *Dst* index service (<http://wdc.kugi.kyoto-u.ac.jp/dst/dir/>).

- 5 From the list, the first 16 events were eliminated due to incomplete information. Among the remain events, 33% were preceded by geomagnetic storm main phase ($Dst < -50\text{nT}$). Thus 80 events were analyzed in this work, because we selected the events classified as pure HILDCAAs, i.e., events not preceded by any geomagnetic storm main phase.

As data sets, the high time-resolution (1 minute) *AE* indices were analyzed to study the dynamical characterization of the HILDCAA events by the RQA method. To eliminate any marginal influences, we considered a 2280 minute interval centered
10 at the middle point of a HILDCAA event. This number of records was determined by the least interval among the events.

For a quantitative comparison of disturbance geomagnetic regimes, we also performed the same RQA during the geomagnetically quiet period listed in Table 1. The quiet days follow the criteria: $Kp \leq 3^0$, $Dst \geq -50\text{ nT}$, and $AE \leq 300\text{ nT}$. The planetary three-hour-range *Kp* index was introduced by J. Bartels in 1949 and designed to be sensitive to any geomagnetic disturbance affecting the Earth ([http://www.gfz-potsdam.de/en/section/earths-magnetic-field/data-products-services/kp-index/](http://www.gfz-potsdam.de/en/section/earths-magnetic-field/data-products-services/kp-index/explanation/)
15 explanation/). It completes a set of indices to diagnose the level of geomagnetic disturbance in a global sense. The geomagnetic indices can be obtained from Word Data Center, Kyoto, in <http://wdc.kugi.kyoto-u.ac.jp/wdc/Sec3.html>. That way, if any, different physical regimes allowed us to verify a distinct characterization of the signals. In our case, periods of HILDCAA events that alter a little bit the physical regime of electrodynamical coupling between solar wind and magnetosphere existing in geomagnetically quiet times.

20 4 Results

As examples of the treatments developed here, two typical cases are shown. First, Fig. 1 shows *AE* variations during a HILDCAA interval. The HILDCAA started at 1734 UT on 30 May (day 150) and continued till 0934 UT on 03 June (day 153) of 1986, with a total duration of about 64 hours. This is shown by a double arrow horizontal line. For the RQA we consider the 2280 minute interval centered at the middle of the HILDCAA. For the identification, two vertical dotted lines mark this
25 interval. Second, Fig. 2 shows *AE* variations during a geomagnetically quiet period. The plot shows the geomagnetically quiet period from 17 to 22 July (day 198 to day 203) of 2006 (from Table 1). The region between the two vertical dotted lines shows the same 2280 minute interval selected for the RQA study as in the HILDCAA case.

The *AE* plots show differences in the amplitudes between the HILDCAA interval (peak about 1200 nT) and the quiet time interval (peak about 300 nT), as expected. However, the behaviors are quite similar.

- 30 Figure 3 represents the space state plots for the HILDCAA and Fig. 4 for the quiet interval shown by the vertical dotted lines in the earlier Figures, respectively. The time delays (τ) used are 34 minutes. The estimated values are determined by the mutual information methodology. The state space charts present snapshots of the interconnections of the records for each case.



Although the amplitudes for the HILDCAA and the quiet period signals are different, the signal patterns are similar in both cases.

We have constructed the space state charts for all 80 HILDCAA intervals and 6 quiet intervals under study. For all the cases, the estimated values of the basic RQA parameters are as follows: The embedded dimension (m) using the false nearest neighbor method was found to be around 6, the time delay (τ) was 34 minutes. The cut-off distance (ϵ) was 30 nT for the HILDCAAs, and ≈ 10 nT for the quiet intervals. The method of ϵ estimation is based on the additive effects of the data resolution and a gaussian noise threshold.

Figure 5 shows the RPs for the HILDCAA and Fig. 6 for the quiet interval. Here we take the embedded dimension (m) and the time delay (τ) equal to 1. These take into account the categorization purpose of the present work, and they do not disturb our characterization process (Iwanski and Bradley, 1998; March et al., 2005; Marwan, 2011). The RPs highlight the recurrences in the signal records showing a slight difference in the dynamical patterns between the HILDCAA interval and the quiet period. To the both systems, the analyses on the large scale patterns in the plots, designated as typology, denote that they are of the disrupted kind, i.e., with abrupt changes in the representation of the dynamics. However, the analysis on the small scale patterns, designated as texture, denote a more complex dynamics to the HILDCAA event than the one to the quiet interval.

The RQA dynamical parameters for this case of HILDCAA are: $RR = 0.0021$, $DET = 0.044$, $LAM = 0.069$, and $ENTR = 0.147$. For the quiet time interval, the parameters are: $RR = 0.0203$, $DET = 0.357$, $LAM = 0.518$, and $ENTR = 0.719$. Clearly, the values of the parameters are about one order of magnitude smaller for the HILDCAA than the values for the quiet interval.

We have performed the same methodology for all the HILDCAAs and geomagnetically quiet intervals under study. The values of the RQA dynamical variables were obtained for each case. The minimum, maximum, mean, standard deviation, median, and mode values are estimated separately for the HILDCAAs and the quiet periods (shown in Table 2). For instance, there is a difference of one order of magnitude between the cases for the mean values. For minima and maxima, the differences are between half and one order of magnitude. The standard deviation, median, and mode are in agreement of characteristic distribution for the phenomena.

Patterns in the signals for the HILDCAA events help to identify the common basic physical features. Figure 7 shows the RQA dynamical parameters for all events under study. For each parameter, we normalized the values for all events with respect to extreme values obtained for the parameter. The empty circles represent the HILDCAA events and the plus signs show the quiet periods. A clear distinction between the HILDCAA events and quiet-time intervals may be noted from the figure. The separation of the results for the HILDCAA event and the quiet time interval establishes a clustering of the results, which characterize two well defined physical regimes.

From the comparison of results obtained using RQA between HILDCAAs and geomagnetically quiet intervals, the physics scenario could be properly interpreted according to a basic view. Although there was an expectation on this interpretation, the quantitative study indicated that in a clear way (the categorization showed in Fig. 7). During HILDCAA events, the two primary electrodynamic interactions (magnetic reconnection and viscous interaction) with transfer of energy and particles are indeed



happening. In principle, interplanetary phenomena producing both of those coupling mechanisms, as processes examined in (Ma et al., 2014), concern the mechanisms related to interplanetary Alfvén waves. During its occurrence, a kind of magnetic disturbance and particle energy deposition can be primarily detected by magnetometers at the polar regions, as the HILDCAA events. Although they can be clearly noticed at high latitudes, those disturbances are weak world-wide manifestations. During geomagnetically quiet conditions, the predominant interaction is the ram pressure on the solar front side of magnetosphere and the development of viscous interaction at flanks. Then we have the proper conditions of transitions from quiescent conditions to weaker geomagnetic disturbances inside the magnetosphere and ionosphere system, as identified by the RQA results. Those RQA features can be an useful characterization for other study purposes.

Thus, in a complementary way, non linear analyses on the dynamics contained in the measurement could help in the evaluation of results developed by computational simulations, such as Ma et al. (2014), Chen et al. (2004), or similar work. With the present work, we have noticed the potential applicability of the RQA method for characterization of various nonlinear geomagnetic processes related to these phenomenology.

5 Conclusions

Using features of non linear system analysis as a hint, a physical scenario could be rebuilt with the aid of the Recurrence Quantification Analysis information extracted from the Recurrence Plot calculation. We performed the same methodology for 80 HILDCAAs and 6 geomagnetically quiet intervals under study. The values of the RQA dynamical variables (RR, DET, LAM and ENTR) characterized the signature related to the HILDCAA processes measured on ground by magnetometers and quantified by the geomagnetic indices AE .

The conclusions are summarized as follows:

- There is a clustering of HILDCAA signatures identified by Recurrence Quantification Analysis. It corroborates the HILDCAA events, described in Tsurutani and Gonzalez (1987), as well defined processes, i.e. unique processes, responsible for the complex transfer of energy and particles from the solar wind plasmas into the magnetosphere-ionosphere system.
- The application of the method indicated, as supported by an expected basic view, the HILDCAA signatures as result of the concurrent magnetospheric processes (magnetic reconnection and viscous interaction).
- Considering proper conditions from transitions from quiescent conditions to weaker geomagnetic disturbances, the quantifications of signals by the RQA method could be useful as characterizations to aid in the MHD studies dealing with processes driven by Alfvén waves.

Also, with this work, we reinforce the potential applicability of the RQA method for characterization of various nonlinear geomagnetic processes related to these phenomenology.



Author contributions. All authors discussed the idea and the approach for the work development and took part in the preparation of the manuscript. O. Mendes and M. O. Domingues worked also in the application of the methodology.

Competing interests. The authors declare that they have no conflict of interest.

Acknowledgements. M.O.D. and O.M. would like to thank the MCTI/FINEP (CT-INFRA 0112052700) and FAPESP (2015/25624-2) for the financial support. O.M., M.O.D. and E.E. would also like to thank the Brazilian CNPq agency (CNPq 312246/2013-7, 306038/2015-3 and 301233/2011-0, respectively) for financial support. R.H. would like to thank the FAPESP 2012/00280-0 for a postdoctoral research fellowship at INPE. V.E.M. would like to thank the MCTI-PCI program (Proc. 455097/2013-5), the research fellowship at INPE. The authors would like to thank the team of Interdisciplinary Center for Dynamics of Complex Systems, University of Potsdam, for the RQA tools (tocsy.pik-potsdam.de), OMNIweb Service (<http://omniweb.gsfc.nasa.gov/>) by NASA and the World Data Center for Geomagnetism, Kyoto, Japan (<http://wdc.kugi.kyoto-u.ac.jp/>), where the geomagnetic indices used in this study were collected from.



References

- Belcher, J. W. and Davis, L. J.: Large-amplitude Alfvén waves in the interplanetary medium: 2, *J. Geophys. Res.*, 76, 3534–3563, 1971.
- Burch, J. L. and Drake, J. F.: Reconnecting magnetic fields, *Am. Sci.*, 97, 392–399, 2009.
- Campbell, W. H.: Introduction to geomagnetic fields, Cambridge, 2003.
- 5 Chen, Q., Otto, A., and Lee, L. C.: Tearing instability, Kelvin-Helmholtz instability, and magnetic reconnection, *J. Geophys. Res.*, 430, 1755–1758, 2004.
- Cover, T. M. and Thomas, J. A.: Elements of Information Theory, Wiley-Interscience, New Jersey, 2006.
- Dungey, J. W.: Interplanetary magnetic field and the auroral zones, *Phys. Rev. Lett.*, 6, 47–48, 1961.
- Echer, E., Gonzalez, W. D., Tsurutani, B. T., and Kozyra, J. U.: High speed stream properties and related geomagnetic activity during the
10 whole heliospheric interval, *Sol. Phys.*, doi:10.1007/s11207-011-9739-0, 2011.
- Echer, E., Tsurutani, B. T., and Gonzalez, W. D.: Extremely low geomagnetic activity during the recent deep solar cycle minimum, *Proc. Int. Astron. Union*, 7, 200–209, doi:10.1017/S17439213120048X, 2012.
- Eckmann, J. P., Kamphorst, S., and Ruelle, D.: Recurrence plots of dynamical systems, *Europhys. Lett.*, 4, 973–977, 1987.
- Gonzalez, W. D. and Mozer, F. S.: A quantitative model for the potential resulting from reconnection with an arbitrary interplanetary magnetic
15 field, *J. Geophys. Res.*, 79, 4186–4194, 1974.
- Gonzalez, W. D., Guarnieri, F. L., Clua-Gonzalez, A. L., Echer, E., Alves, M. V., Ogino, T., and Tsurutani, B. T.: Recurrent Magnetic Storms: Corotating Solar Wind Streams, chap. Magnetospheric energetics during HILDCAAs, AGU, doi:10.1029/167GM15, 2006.
- Guarnieri, F. L.: Recurrent Magnetic Storms: Corotating Solar Wind Streams, chap. The nature of auroras during high-intensity long-duration continuous AE activity (HILDCAA) events: 1998–2001, AGU, doi:10.1029/167GM19, 2006.
- 20 Guarnieri, F. L., Tsurutani, B. T., Gonzalez, W. D., Clua-Gonzalez, A. L., Grande, M., Soraas, F., and Echer, E.: ICME and CIR storms with particular emphases on HILDCAA events, in: ILWS WORKSHOP 2006, COSPAR, GOA, India, 2006.
- Hajra, R., Echer, E., Tsurutani, B. T., and Gonzalez, W. D.: Solar cycle dependence of high-intensity long-duration continuous AE activity (HILDCAA) events, relativistic electron predictors?, *J. Geophys. Res.*, 118, doi:10.1002/jgra.50530, 2013.
- Hajra, R., Echer, E., Tsurutani, B. T., and Gonzalez, W. D.: Superposed epoch analyses of HILDCAAs and their interplanetary drivers: solar
25 cycle and seasonal dependences, *J. Atmos. Sol. Terr. Phys.*, 121, doi:10.1016/j.jastp.2014.09.012, 2014a.
- Hajra, R., Echer, E., Tsurutani, B. T., and Gonzalez, W. D.: Solar wind-magnetosphere energy coupling efficiency and partitioning: HILDCAAs and preceding CIR storms during solar cycle 23, *J. Geophys. Res.*, 119, doi:10.1002/2013JA019646, 2014b.
- Hajra, R., Tsurutani, B. T., Echer, E., and Gonzalez, W. D.: Relativistic electron acceleration during high-intensity, long-duration, continuous AE activity (HILDCAA) events: solar cycle phase dependences, *Geophys. Res. Lett.*, 41, doi:10.1002/2014GL059383, 2014c.
- 30 Hajra, R., Tsurutani, B. T., Echer, E., Gonzalez, W. D., Brum, C. G., Vieira, L. E. A., and Santolik, O.: Relativistic electron acceleration during HILDCAA events: are precursor CIR magnetic storms important?, *Earth, Planets Space*, doi:10.1186/s40623-015-0280-5, 2015a.
- Hajra, R., Tsurutani, B. T., Echer, E., Gonzalez, W. D., and Santolik, O.: Relativistic ($E > 0.6$, > 2.0 , and > 4.0 mev) electron acceleration at geosynchronous orbit during high-intensity, long-duration, continuous AE activity (HILDCAA) events, *Astrophys. J.*, 799, doi:10.1088/0004-637X/799/1/39, 2015b.
- 35 Hargreaves, J. K.: The solar-terrestrial environment, Cambridge, 1992.
- Hasegawa, H., Fujimoto, M., Phan, T. D., Rème, H., Balogh, A., Dunlop, M. W., Hashimoto, C., and TanDokoro, R.: Transport of solar wind into Earth's magnetosphere through rolled-up Kelvin-Helmholtz vortices, *Nature*, 102, 151–161, 1997.



- Horne, R. B.: Rationale and requirements for a european space weather programme, in: Space Weather Workshop: Looking Towards a European Space Weather Programme, pp. 139–144, European Space Agency, Noordwijk, The Netherlands, 2003.
- Iwanski, J. S. and Bradley, E.: Recurrence plots of experimental data: to embedded or not to embed?, *Chaos*, 8, 861–871, 1998.
- Kivelson, M. G. and Russell, C. T., eds.: Introduction to Space Physics, Cambridge, 2 edn., 1995.
- 5 Kozyra, J. U., Crowley, G., Emery, B. A., Fang, X., Maris, G., Mlynczak, M. G., Niciejewski, R. J., Palo, S. E., Paxton, L. J., Randall, C. E., Rong, P. P., Russell, J. M., Skinner, W., Solomon, S. C., Talaat, E., Wu, Q., and Yee, J. H.: Recurrent Magnetic Storms: Corotating Solar Wind Streams, chap. Response of the upper/middle atmosphere to coronal holes and powerful high-speed solar wind streams in 2003, AGU, doi:10.1029/167GM24, 2006.
- Ma, X., Otto, A., and Delamere, P. A.: Interaction of magnetic reconnection and kelly-helmholtz modes for large magnetic shear: 1. kelly-helmholtz trigger, *J. of Geophys. Res., Space Physics*, 119, 781—797, doi:10.1002/2013JA019224, 2014.
- 10 Maizel, J. V. and Lenk, R. P.: Enhanced graphic matrix analysis of nucleic acid and protein sequences, *Genetic*, 78, 7665–7669, *proc. Natl. Acad. Sci. USA*, 1981.
- March, T. K., Chapman, S. C., and Dendy, R. O.: Recurrence plot statistics and the effect of embedding, *Phys. D*, 200, 173–184, 2005.
- Marwan, N.: Encounters with neighbours. current developments of concepts based on recurrence plots and their applications, Ph.D. thesis, Institut Für Physik, Fakultät Mathematik und Naturwissenschaften, Universität Potsdam., 2003.
- 15 Marwan, N.: How to avoid potential pitfalls in recurrence plot based data analysis, *Int. J. Bifurcation Chaos*, 21, 1003, 2011.
- Marwan, N. and Kurths, J.: Nonlinear analysis of bivariate data with cross recurrence plots, *Phys. Lett. A*, 302, 299–307, doi:http://dx.doi.org/10.1016/S0375-9601(02)01170-2, 2002.
- Marwan, N. and Webber, C. L. J.: Recurrence Quantification Analysis, chap. Mathematical and computational foundations of recurrence quantifications, pp. 3–43, Springer, 2015.
- 20 Marwan, N., Carmen, M., Romano, M. T., and Kurths, J.: Recurrence plots for the analysis of complex systems, *Phys. Reports*, 438, 237–329, doi:http://dx.doi.org/10.1016/j.physrep.2006.11.001, 2007.
- Mendes, O., Domingues, M. O., and da Costa, A. M.: Introduction to planetary electrodynamics: a view of electric fields, currents and related magnetic fields, *Advances in Space Research*, 35, 812–828, doi:http://dx.doi.org/10.1016/j.asr.2005.03.139, 2005.
- 25 Menk, F. and Waters, C. L.: Magnetoseismology, Wiley-VCH, 1 edn., 2013.
- Schulman, L. S.: Note on the quantum recurrence theorem, *Phys. Rev. A*, 18, 2379–2380, 1978.
- Shannon, C. E.: The Mathematical Theory of Communication, University of Illinois, Urbana, IL, University of Illinois, Urbana, IL, 1964.
- Takens, F.: Dynamical Systems and Turbulence, Warwick 1980, vol. 898, chap. Detecting strange attractors in turbulence, pp. 366–381, Springer Berlin Heidelberg, Berlin, doi:10.1007/BFb0091924, 1981.
- 30 Trulla, L. L., Giuliani, A., Zbilut, J. P., and Webber, C. L. J.: Recurrence quantification analysis of the logistic equation with transients, *Physics Letters A*, 223, 255–260, 1996.
- Tsurutani, B. T. and Gonzalez, W. D.: The cause of High-Intensity, Long-Duration, Continuous AE Activity (HILDCAAs): interplanetary Alfvén wave trains, *Planet. Space Sci.*, 35, 405, 1987.
- Tsurutani, B. T., Gould, T., Goldstein, B. E., Gonzalez, W. D., and Sugiura, M.: Interplanetary Alfvén waves and auroral (substorm) activity: IMP 8, *J. Geophys. Res.*, 95, 2241–2252, doi:10.1029/JA095iA03p02241, 1990.
- 35 Tsurutani, B. T., Ho, C., Smith, E. J., Neugebauer, M., Goldstein, B. E., Mok, J. S., Arballo, J. K., Balogh, A., Southwood, D. J., and Feldman, W. C.: The relationship between interplanetary discontinuities and Alfvén waves: Ulysses observations, *Geophys. Res. Lett.*, 21, 2267–2270, doi:10.1029/94GL02194, 1994.



- Tsurutani, B. T., Gonzalez, W. D., Clua-Gonzalez, A. L., Tang, F., Arballo, J. K., and Okada, M.: Interplanetary origin of geomagnetic activity in the declining phase of the solar cycle, *J. Geophys. Res.*, 100, 21,717–21,733, 1995.
- Tsurutani, B. T., Gonzalez, W. D., lua-Gonzalez, A. L., Guarnieri, F. L., Gopalswamy, N., Grande, M., Kamide, Y., Kasahara, Y., Mann, I., Lu, G., McPherron, R., Soraas, F., and Vasyliunas, V.: Corotating solar wind streams and recurrent geomagnetic activity: a review, *J. Geophys. Res.*, 111, A07S01, doi:10.1029/2005JA011273, 2006.
- 5 Tsurutani, B. T., Echer, E., and Gonzalez, W. D.: The solar and interplanetary causes of the recent minimum in geomagnetic activity (MGA23): a combination of midlatitude small coronal holes, low IMF Bz variances, low solar wind speeds and low solar magnetic fields, *Ann. Geophys.*, 29, 839–849, 2011a.
- Tsurutani, B. T., Echer, E., Guarnieri, F. L., and Gonzalez, W. D.: The properties of two solar wind high speed streams and related geomagnetic activity during the declining phase of solar cycle 23, *J. Atmos. Sol. Terr. Phys.*, 73, 164–177, 2011b.
- 10 Webber Jr., C. L. and Zbilut, J. P.: Dynamical assessment of physiological systems and states using recurrence plot strategies, *J. Appl. Physiol.*, 76, 965–973, 1994.
- Wrenn, G. L.: Conclusive evidence for internal dielectric charging anomalies on geosynchronous communications spacecraft, *J. Spacecraft Rockets*, 32, 514–520, 1995.
- 15 Zbilut, J. P. and Webber Jr., C. L.: Embeddings and delays as derived from quantification of recurrence plots, *Phys. Lett. A*, 171, 199–203, 1992.

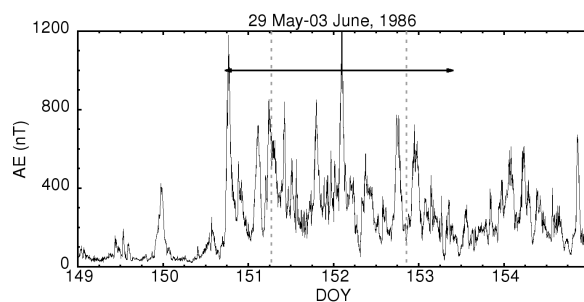


Figure 1. As example, the geomagnetic AE index during the HILDCAA event on 29 May (DOY 150) - 03 June (153) 1986. The HILDCAA interval is identified by the double arrow horizontal line, and the AE interval used for the RQA is between the vertical dotted lines.

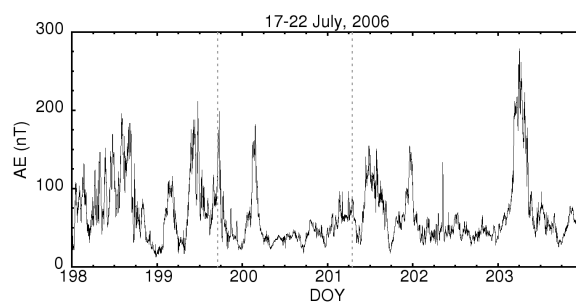


Figure 2. As example, the geomagnetic AE index during the geomagnetically quiet period on 17 (DOY 198) - 22 (203) July 2006. The AE interval used for the RQA is between the vertical dotted lines.

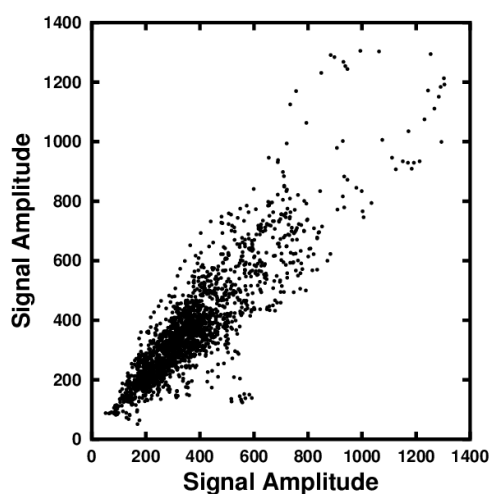


Figure 3. The space state representation for the HILDCAA example. The signal corresponds to the region shown by the vertical dotted lines in Figure 1. The delay time is 34 minutes.

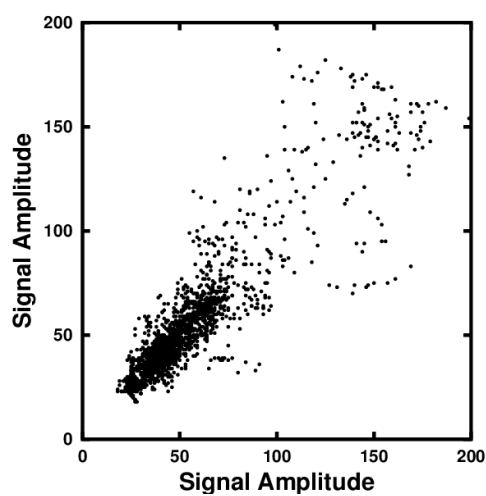


Figure 4. The space state representation for the geomagnetically quiet period example. The signal corresponds to the region shown by the vertical dotted lines in Figure 2. The delay time is 34 minutes.

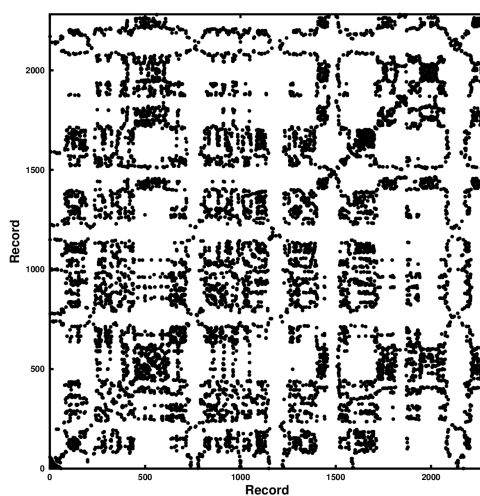


Figure 5. The recurrence plot for the HILDCAA example. The interval shown by the vertical dotted lines in Figure 1 is used to obtain the plot.

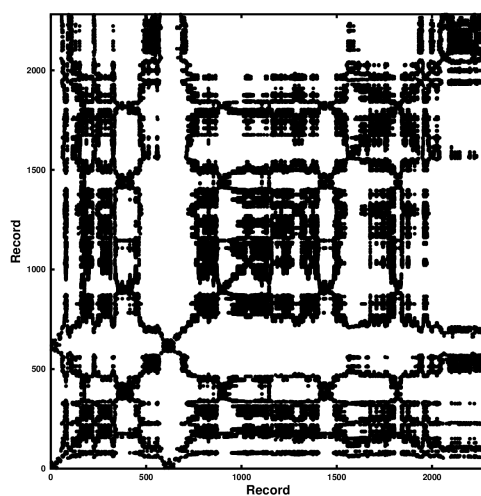


Figure 6. The recurrence plot for the geomagnetically quiet period example. The interval shown by the vertical dotted lines in Figure 2 is used to obtain the plot.

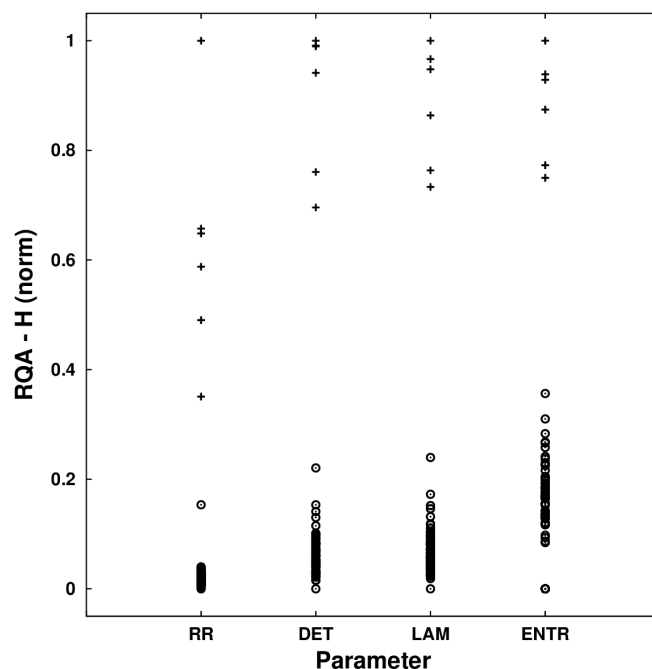


Figure 7. Normalized representation of the RQA parameters for HILDCAA events (o) and the geomagnetically quieter intervals (+).



Table 1. The geomagnetically quiet intervals

Date	$Kp \leq$	$AE \leq$	$Dst \geq$
14 - 18 November 2000	3^0	267 nT	-20 nT
26 - 30 November 2001	3^-	133 nT	-50 nT
19 - 25 June 2004	2^0	167 nT	0 nT
19 - 27 June 2006	2^0	167 nT	-9 nT
15 - 23 July 2006	2^0	200 nT	32 nT
01 - 09 December 2007	3^0	200 nT	-5 nT



Table 2. The Recurrence Quantification Analysis results

Value	HILDCAA period				geomagnetically quiet interval			
	RR	DET	LAM	ENTR	RR	DET	LAM	ENTR
Min	0.0010	0.010	0.014	0.000	0.0115	0.251	0.397	0.574
Max	0.0056	0.086	0.139	0.273	0.0307	0.357	0.536	0.766
Mean	0.0016	0.031	0.049	0.091	0.0195	0.321	0.473	0.672
Std	0.0005	0.012	0.020	0.073	0.0065	0.046	0.058	0.075
Med	0.0015	0.028	0.046	0.104	0.0194	0.345	0.487	0.690
Mod	0.0013	0.010	0.014	0.000	0.0115	0.251	0.397	0.574